

## Development and Application of 3D Loading Model Test System of Underground Cavern

Leyang Zheng<sup>1,2,\*</sup>, Qiangyong Zhang<sup>1</sup>, Qiang Gao<sup>1</sup>, Liqiang Wang<sup>1</sup>, Xun Zhao<sup>1</sup>

<sup>1</sup>Shandong University, Shandong, China.

<sup>2</sup>Shandong Shixin Construction Co.Ltd, Shandong, China.

\*Email: 868389126@qq.com

### Abstract

With global economic development, shallow resources on the earth peter out. Which results in resource development moving toward deep within the earth. Meanwhile, survival development demand of human beings and exploration of unknown world also expand underground activity space constantly. As excavation depth of underground cave increases, there is huge difference between mechanical properties of deep rock mass and that of deep rock mass on the condition of “three highs and one disturbance”, and it usually brings about many unforeseeable problems. To solve deficiencies of existing model test system, Shandong University Geotechnical Engineering Center develops UHP intelligent NC true 3D gradient loading test. Nominal output of system is 63 MPa, maximum load is 45 000 kN, the system can realize any load ranging from 0.05MPa to 62MPa. In this paer, 3D geomechanics model test is made for formation process of ancient karst cave with super-depth reservoir in Sichuan Fengjiang Oilfield through UHP intelligent NC true 3D loading model test system to verify the validity of the system.

### Keywords

List 3D Loading Model Test System, Underground cavern, Engineering application.

### 1. Introduction

With rapid development of global economy, shallow resources on the earth peter out. Which results in resource development moving toward deep within the earth. Meanwhile, survival development demand of human beings and exploration of unknown world also expand underground activity space constantly. In the perspective of resource and energy development, nowadays, mining depth of coalmine resources has reached 1500m, mining depth of geothermal resources has exceeded 3000m, mining depth of nonferrous metal mine has exceeded 4350m, and mining depth of oil gas energy has reached 7500m. As excavation depth of underground cave increases, there is huge difference between mechanical properties of deep rock mass and that of deep rock mass on the condition of “three highs and one disturbance”, and it usually brings about many unforeseeable problems, such as zonal disintegration, large deformation, rockburst, rock burst, etc. Now, it has been inappropriate to study nonlinear failure problem of deep rock mass using traditional theory, method and technology of shallow rock mass, and it is urgent to make an in-depth research on nonlinear deformation failure mechanism of surrounding rock of deep cavern. Compared with deficiencies of theoretical analysis and numerical computation in simulating cavern failure mechanism, geomechanics model test becomes an important approach to study nonlinear deformation failure law of surrounding rock of deep and super-depth underground cavern by virtue of its vividness, visuality and trueness.

Geomechanics model test requires possession of model test system. So far, current research situation about geomechanics model test system is below: Li Zhongkui et. al. developed a discrete 3D multi-

principal stress surface loading test system, and made a geomechanics model test of underground powerhouse cavern for Xiluodu Hydropower Station; Chen Anmin et. al. developed multi-function simulation test device of YD-A geotechnical engineering, and made a model test of underground powerhouse cavern for Xiaolangdi Hydropower Station; Jiang Yaodong et. al. developed true three-axis planar model test system of roadway, and made a physical model test of stable roadway on complicated conditions; Zhang Qiangyong et. al. developed composite geomechanics model test system, and made a 3D geomechanics model test of turnout tunnel of Hurongxi Expressway; Zhu Weishen et. al. developed quasi-3D model test bed device, and made a physical model test of underground housepower cavern excavation of Shuangjiangkou Hydropower Station.

For deformation failure process of super-depth underground cavern with depth above 5000m, a physical model test is required. So far, existing geomechanics model test system has obvious deficiencies: (1) Nominal output of the model system is limited, so the system is difficult to simulate deformation failure law of deep cavern on UHP ground stress condition; (2) most model test system considers uniform loading, and they are difficult to simulate heterogeneous distribution of deep ground stress; and (3) model test is difficult to monitor real-time displacement change in any positions inside model dynamically and automatically.

## 2. Introduction of UHP intelligent NC true 3D loading model test system

UHP intelligent NC true 3D loading model test system is mainly made up of model counterforce rack, UHP loading system, intelligent hydraulic control system, automatic model displacement acquisition system and HD multi-probe model peep system (See Fig. 1). Model test counterforce rack is mainly used for accommodating test model and as counterforce device of model loading. It has such advantages as high stiffness, good integral stability, convenient model excavation and easy failure phenomenon observation. UHP loading system is arranged inside model counterforce rack. It is mainly made up of 33 hydraulic jacks with designed tonnage 5000kN, bench-type force loading module and one set of 3D loading guide frame. It is mainly used for UHP true 3D loading of test model. Intelligent hydraulic control system exposes gradient heterogeneous loading on model through NC technology. Automatic model displacement acquisition model monitors displacement of any position inside model automatically using photoelectric conversion technology, and displacement measurement accuracy reaches 0.001mm. HD multi-probe peep of model, using HD camera shooting technology, realizes real-time dynamic peep of model cave deformation failure process through transparent window set on the obverse side of model counterforce rack.



Fig. 1 UHP intelligent NC true 3D loading model test system

### 3. Engineering application

Taking super-depth carbonate reservoir karst cave in Sichuan Fengjiang Oilfield as research background, the author makes a 3D geomechanics model test against super-depth reservoir karst cave formation collapse failure process.

#### 3.1 Project profile

Sichuan Fengjiang Oilfield is a typical Ordovician super-depth carbonate reservoir, the burial depth of reservoir is 5300m to 6200m, and many ancient karst caves have been distributed during the formation of reservoir. The dimension of karst caves varies from several meters to several dozen meters, and they are main oil storage space of oilfield. During reservoir development, deep karst cave collapse failure phenomenon is observed to occur during production of some oil wells, which affects oil well yield seriously. To analyze the impact of karst cave collapse failure on oil well recovery ratio, it is necessary to understand and disclose collapse failure mechanism of karst caves during formation and oil recovery of ancient karst caves so as to provide scientific basis for optimizing petroleum mining technology. To this end, a model test is carried out against cavern collapse failure caused by formation of karst caves are carried out in this paper. The karst cave formation collapse failure model test has been completed, so the test result of model becomes the important content to be expounded in the paper, while model test of karst cave collapse failure caused by petroleum mining is to be carried out and it will be expounded additionally after completion of the test.

#### 3.2 Model simulation material

A large indoor 3D geomechanics model test is made against formation collapse failure process of calcific rectangular karst cave at 5600m burial depth of Sichuan Fengjiang Oilfield using UHP intelligent NC true 3D loading model test system developed in this paper, and formation process of model cave adopts manual drilling. Geometric similitude ratio of model is  $CL = LP/LM = 50$ , dimension of test model is 1 500 mm×1 500mm×500 mm, sectional dimension of rectangular karst cave is 200 mm×200 mm (see Fig. 2). Table 1 is physical and mechanical parameters of rock carbonate rock.

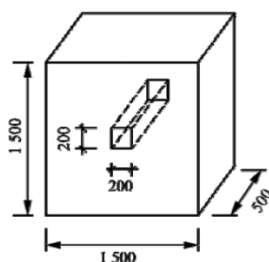


Fig. 2 Dimension of test model

Table 1 Physical and mechanical parameters of primary carbonate rock

| Volume Weight<br>( $\text{kN} \cdot \text{m}^{-3}$ ) | Modulus of Deformation<br>/MPa | Compressive Strength<br>/MPa | Tensile Strength<br>/kPa | Cohesion<br>/kPa | Internal Friction Angle<br>/ $^{\circ}$ | Poisson's Ratio |
|--|--------------------------------|------------------------------|--------------------------|------------------|---|-----------------|
| 27   | 36                             | 74                           | 3.8                      | 12               | 36                                      | 0.25            |

Geometric similitude ratio of model is  $CL = LP/LM = 50$  and volume-weight similitude ratio of model is  $C_\gamma = 1$ , so it is known according to similarity conditions of model: similitude ratio of strain, Poisson's ratio and internal friction angle of model is  $C_\varepsilon = C_\mu = C_\phi = 1$ ; similitude ratio of stress, cohesion and modulus of deformation of model is  $C_\sigma = C_c = C_E = 50$ . Therefore, we get theoretical value of physical and mechanical parameters of model simulation material. See Table 2.

Table 2 Theoretical value of physical and mechanical parameters of model simulation material

| Volume Weight<br>( $\text{kN} \cdot \text{m}^{-3}$ ) | Modulus of Deformation<br>/MPa | Compressive Strength<br>/MPa | Tensile Strength<br>/kPa | Cohesion<br>/kPa | Internal Friction Angle<br>/ $(^\circ)$ | Poisson's Ratio |
|--|--------------------------------|------------------------------|--------------------------|------------------|---|-----------------|
| 27   | 720                            | 1.48                         | 76                       | 240              | 36                                      | 0.25            |

According to theoretical value of physical and mechanical parameters of model simulation material in Table 2, on a basis of iron ore concentrate cementing rock soil simulation material ratio, we adjust material ratio and make related mechanical test, and finally get model simulation material ratio (See Table 3) and test value of physical and mechanical parameters of model simulation material obtained from test according to such ratio (See Table 4).

Table 3 Model simulation material ratio

| Material Ratio | Molarity of Cementing Agent | Cementing Agent Ratio in the Material |
|----------------|-----------------------------|---------------------------------------|
| 1:0.67:0.25    | 18                          | 6.5                                   |

Table 4 Test value of physical and mechanical parameters of model simulation material

| Volume Weight<br>( $\text{kN} \cdot \text{m}^{-3}$ ) | Modulus of Deformation<br>/MPa | Compressive Strength<br>/MPa | Tensile Strength<br>/kPa | Cohesion<br>/kPa | Internal Friction Angle<br>/ $(^\circ)$ | Poisson's Ratio |
|--|--------------------------------|------------------------------|--------------------------|------------------|---|-----------------|
| 26.8~27.1  | 660~750                        | 1.38~1.61                    | 71~82                    | 226~263          | 35.4~36.5                               | 0.23~0.26       |

According to Table 4, it is known physical and mechanical parameters of model material allocated according to material ratio is similar with that of primary rock. Therefore, the model material with such ratio could be used for geomechanics model test.

### 3.3 Model making method

Test model is made using laminated paving compaction method. Specific processes are: prior to making test model, determine layers of materials required by model entity making and thickness of each layer; then, compute material dosage of each layer according to material ratio in Table 3, pour the evenly mixed material to model rack and pave it evenly, compact model material by layers according to pressure of model material specimen making; then, air dry compacted material by layers using a big-power fan so that alcohol solvent in the model totally volatilized; later, lay minitype multipoint displacement meter, minitype earth pressure cell, strain brick and other test sensors successively at designed elevation. After a layer of test instruments are laid, we prepare and mix next

layer of model material → pave by layers → compact by layers → air dry by layers → lay measuring elements for positioning until completion of model marking.

To eliminate interface formed among material layers we must splash alcohol on the last layer of compacted material before paving material each time, and rake the surface of last layer of compacted material to loosen it. Then, we pave and compact next layer of material to ensure no interface formed between laminated materials.

### 3.4 Model test method

To observe rectangular karst cave formation collapse failure law, measuring elements are laid around model cavern used for observing displacement, strain and stress of model. Fig. 3 is model observation section layout diagram. Where, I-I section is allocated with DZ-I resistance strain soil pressure cell to observe model stress change law, the dimension of pressure cell is 17 mm×7mm, and the range is 1.0MPa; II-II section is allocated with minitype multipoint displacement meter to observe model displacement change law; and III-III section is allocated with minitype strain brick to observe model strain change law.

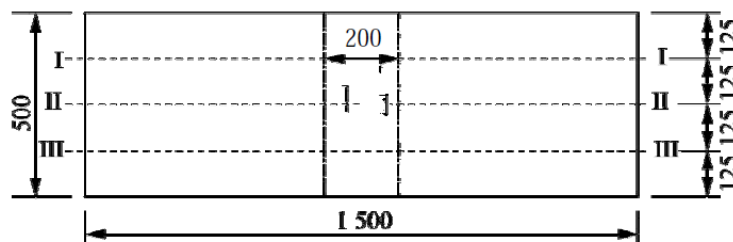


Fig. 3 Model observation section (unit: mm)

### 3.5 Model loading method

To simulate high ground stress environment of super-depth cavern, a 3D gradient heterogeneous loading is imposed on the model entity, as is shown in Fig. 4. According to stress similitude condition  $C_\sigma = C_r C_l = 50$ , actual burial depth of model top is 5600m, loading stress on top surface of model is 3.0MPa; actual burial depth of model bottom is 5675m, and loading stress on bottom surface of model is 3.1MPa; gradient loading is applied to left, right and back side of model as burial depth  $h$  varies according to  $\sigma = \gamma kh$ . Where,  $\gamma$  is volume weight of rock mass,  $k$  is horizontal pressure coefficient of ground stress, and  $k=0.62$ ; passive loading is applied to the front side of model through constraint.

After completing model entity making, boundary stress is applied by levels on the boundary of model entity according to ground stress shown in Fig. 4 until it reaches the design value. Then, at least 24h steady pressure is required so that initial high ground stress field is formed inside model entity. Later, manual drilling mode is adopted along cave axis for segmented excavation until model cavern totally connected. During segmented excavation, deformation failure status of model cavern shall be observed successively.

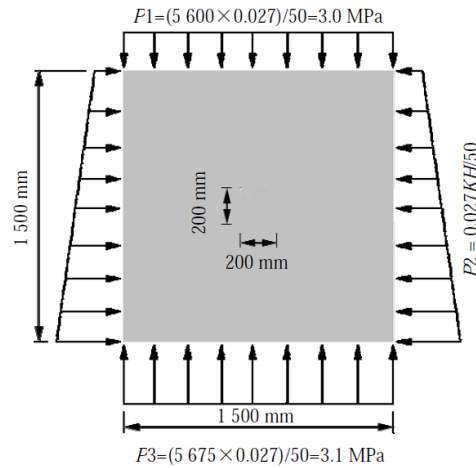
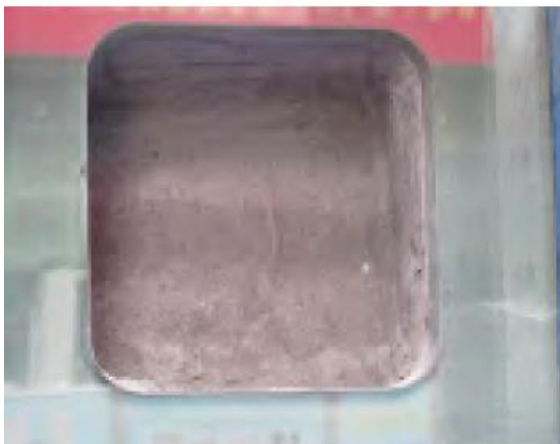


Fig. 4 Model loading scheme

### 3.6 Test result analysis of model

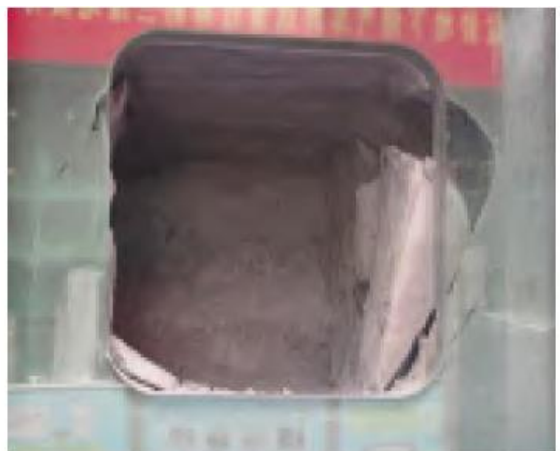
#### 1) Karst cave collapse failure process



Microcrack formed on sidewall of 12.5cm cavern



Shear crack formed on side wall of 25cm cavern



Shear collapse failure formed on right sidewall of 40cm cavern



Wide shear crack formed on left sidewall of 40cm cavern

Fig. 5 is pictures about karst cave collapse failure process.





Fig. 6 Model cave collapse failure process

According to Fig. 6, it is known: during formation of karst cave, microcrack is firstly formed at footing of left and right sidewall of cavern. As time goes, microcrack expands upward along left and right sidewall of cavern and then forms multiple shear cracks. When shear crack expands to cavern roof and forms wide connected crack, it results sidewall collapse failure of cavern in turn. After cavern is fully connected and formed, cavern roof crack is serious and shows sink. Finally, it results in collapse failure of the whole karst cave. Vertical stress of cavern is greater than horizontal stress, so karst cave failure mode is mainly tensile shear failure mode and karst cave sidewall crack surface parallels with maximal vertical principal compressive stress approximately. Finally, V-tensile shear failure surface is formed.

## 2) Change law of displacement around model cave

Fig. 7 is displacement distribution around model cave after formation of karst cave. According to Fig. 7, it is known displacement on cavern roof is relatively great and homogeneous, indicating that karst cave roof moves downward during formation of cavern. The displacement of left and right sidewall

of cavern decreases as the distance from the cavern wall increases. Where, displacement on measured point nearest cavern wall is relatively greatest, indicating that the position near cavern wall is the most serious failure area on the condition of high ground stress burial depth. As it extends outward of cavern, the displacement on the measuring point 460mm from cavern wall is 0, indicating that such position is beyond cavern failure influence scope. Thus, it is known that maximum influence scope of karst cave collapse failure is 2.3 times of cavern span.

3) Change law of stress around model cave

Fig. 8 is radial stress distribution around model cave after karst cave formation. According to Fig. 8, it is known, the nearer the distance from cavern wall is, the more serious the radial stress release around cavern is, and radial stress on the measured point 460mm distance from cavern wall has no change, indicating that such position is beyond of cavern failure influence scope. Thus, it is known that maximum influence scope of karst cave collapse failure is 2.3 times of cavern span.

According to result analysis of the above model test, it indicates that model test system developed by Shandong University Geotechnical Engineering Center has disclosed deformation characteristics and failure law of ancient karst cave with super-depth reservoir during the formation. It lays good foundation for studying karst cave collapse failure mechanism caused by petroleum mining, and also verifies the reliability of the developed model test system effectively.

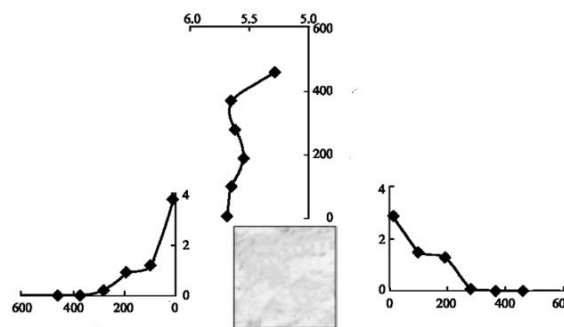


Fig. 7 Displacement distribution around model tunnel

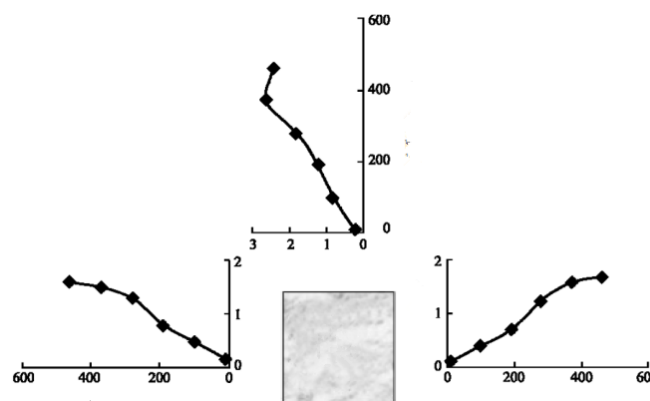


Fig. 8 Radial stress distribution around model tunnel

**4. Conclusion**

1) Through UHP intelligent NC 3D model test system, a 3D geomechanics model test is made for the formation process of ancient karst cave with super-depth reservoir in Sichuan Fengjiang Oilfield. The formation failure process of ancient karst cave reappears in the test. Through the test, the author



obtains nonlinear deformation characteristics and stress change law of karst cave collapse failure and discloses formation collapse failure mechanism of ancient karst cave effectively.

2) Through engineering application, the developed model test system is verified to be reliable. Such system has wide application prospect in studying nonlinear deformation failure mechanism of super-depth underground cavern.

## References

- [1]Li Yang. Development Theory and Method of Carbonate Fracture-Cave Reservoir [J]. Journal of Petroleum Science, 2013, 34(1): P115 to P121.
- [2]Zhang Qiangyong, Li Shucui, Li Yong, et. al. New Method, New Technology and Engineering Application of Underground Engineering Model Test [M]. Science Press, 2012: P64 to P79.
- [3]He Manchao, Xie Heping, Peng Suping, et. al. Study on Deep Mined Rock Mass Mechanics [J]. Chinese Journal of Rock Mechanics and Engineering, 2005, 24(16): P2803 to P2813.
- [4]Zhu Jie, Wang Renhe, Lin Bin. Study on Frequent Fracture Phenomena and Fracture Opening of Surrounding Rock of Deep Roadway [J]. Journal of China Coal Society, 2010,35(6): P887 to P890.
- [5]Li Jianfeng, Cheng Jianlong, Feng Chaochao. Zonal Disintegration Simulation Experiment of Surrounding Rock of Deep Soft Rock Roadway [J]. Journal of Liaoning Technical University (Natural Science), 2014,33(03):P298 to P305.
- [6]Zhang Qiangyong, Chen Xuguang, Lin Bo, et. al. Experimental Study on Zonal Disintegration 3D Geomechanics Model of Surrounding Rock of Deep Roadway [J]. Chinese Journal of Rock Mechanics and Engineering, 2009, 28(9): P1757 to P1766.